



Contents lists available at ScienceDirect

Quaternary Science Reviews

journal homepage: www.elsevier.com/locate/quascirev

Paired bedrock and boulder ^{10}Be concentrations resulting from early Holocene ice retreat near Jakobshavn Isfjord, western Greenland

Lee B. Corbett^{a,*}, Nicolás E. Young^b, Paul R. Bierman^a, Jason P. Briner^b, Thomas A. Neumann^c, Dylan H. Rood^{d,e}, Joseph A. Graly^a

^a Department of Geology, University of Vermont, Burlington, VT 05405, USA

^b Department of Geology, State University of New York at Buffalo, Buffalo, NY 14260, USA

^c NASA Goddard Space Flight Center, Greenbelt, MD 20770, USA

^d Center for Accelerator Mass Spectrometry, Lawrence Livermore National Laboratory, Livermore, CA 94550, USA

^e Earth Research Institute, University of California, Santa Barbara, CA 93106, USA

ARTICLE INFO

Article history:

Received 7 February 2011

Received in revised form

29 March 2011

Accepted 1 April 2011

Available online 14 May 2011

Keywords:

Greenland ice sheet

Holocene

Cosmogenic dating

Deglaciation

Erosion

ABSTRACT

We measured *in situ* cosmogenic ^{10}Be in 16 bedrock and 14 boulder samples collected along a 40-km transect outside of and normal to the modern ice margin near Sikujuitsoq Fjord in central-west Greenland (69°N). We use these data to understand better the efficiency of glacial erosion and to infer the timing, pattern, and rate of ice loss after the last glaciation. In general, the ages of paired bedrock and boulder samples are in close agreement ($r^2 = 0.72$). Eleven of the fourteen paired bedrock and boulder samples are indistinguishable at 1σ ; this concordance indicates that subglacial erosion rates are sufficient to remove most or all ^{10}Be accumulated during previous periods of exposure, and that few, if any, nuclides are inherited from pre-Holocene interglaciations. The new data agree well with previously-published landscape chronologies from this area, and suggest that two chronologically-distinct land surfaces exist: one outside the Fjord Stade moraine complex ($\sim 10.3 \pm 0.4$ ka; $n = 7$) and another inside ($\sim 8.0 \pm 0.7$ ka; $n = 21$). Six ^{10}Be ages from directly outside the historic (Little Ice Age) moraine show that the ice margin first reached its present-day position $\sim 7.6 \pm 0.4$ ka. Early Holocene ice margin retreat rates after the deposition of the Fjord Stade moraine complex were $\sim 100\text{--}110$ m yr^{-1} . Sikujuitsoq Fjord is a tributary to the much larger Jakobshavn Isfjord and the deglaciation chronologies of these two fjords are similar. This synchronicity suggests that the ice stream in Jakobshavn Isfjord set the timing and pace of early Holocene deglaciation of the surrounding ice margin.

© 2011 Elsevier Ltd. All rights reserved.

1. Introduction

The measurement of cosmogenic isotopes in morainal boulders and glacially sculpted bedrock surfaces has provided increasingly widespread control on the chronology of deglaciation (Phillips et al., 1990; Fabel and Harbor, 1999; Balco, 2011). Glaciers and ice sheets are sensitive indicators of climate, and respond to changes in precipitation and temperature by expanding and shrinking (IPCC, 2007; Alley et al., 2010). Improved constraints on the timing and pattern of past deglaciation events provides an important context in which to interpret the dynamics of present-day and future ice loss (Long, 2009).

The dating of glacial events with cosmogenic nuclides depends on the veracity of key methodological assumptions: lack of post-depositional erosion or burial and minimal inheritance of nuclides from prior periods of exposure. In recent years, refined analytical and computational techniques have reduced age uncertainty (Hunt et al., 2008; Rood et al., 2010); however, the accuracy of cosmogenic ages still depends on the aforementioned assumptions (Bierman, 1994; Gosse and Phillips, 2001; Heyman et al., 2010). For older glaciations, surface erosion limits the accuracy of ages and results in age underestimates (Smith et al., 2005). Similar age underestimation also results from burial by till or snow cover (Schildgen et al., 2005). Conversely, inheritance of nuclides from prior periods of exposure can lead to age overestimates (Briner and Swanson, 1998). Because erratic boulders and the striated bedrock that underlies them have different pre-exposure histories and different likelihoods of post-exposure burial, a pair-wise comparison of exposure ages provide a useful means to test the assumption of no

* Corresponding author. Tel.: +1 802 656 4411.

E-mail address: Ashley.Corbett@uvm.edu (L.B. Corbett).

inheritance and no burial. However, paired sampling of striated bedrock and erratic boulders has been conducted in only a few places (Marsella et al., 2000; Pallas et al., 2006; Delmas et al., 2008).

Large ice sheets have a variety of different ice margin types and thus can lose mass and retreat in a variety of ways. In some areas, the ice sheet margin is land-based and loses mass through surface melting or sublimation. In areas where the ice sheet margin is floating (marine-based) rather than grounded, mass is lost primarily through calving. For marine-based ice sheets, debris build-up at the glacier's terminus can create an end moraine, which serves to stabilize the ice against further calving (Alley et al., 2007). In some areas, fast-flowing ice streams channelize regional ice flow and transport large volumes of ice to the sea (Bentley, 1987).

Although the deglaciation dynamics of large ice streams is relatively well-studied (Weidick et al., 1990; Long and Roberts, 2002, 2003; Lloyd et al., 2005; Long et al., 2006; Weidick and Bennike, 2007; Young et al., 2011), the influence of such fast-flowing systems on the retreat of adjacent ice margins is not well understood. Western Greenland, where ice streams are juxtaposed with less active ice margins, is an ideal place to study the dynamics of ice retreat in an area adjacent to a major ice stream. Here, we present ^{10}Be data from 16 sites in Sikuijuitsoq Fjord, a tributary fjord of a large, rapidly moving ice stream (Jakobshavn Isbræ; Figs. 1 and 2). Measurements of *in situ* produced cosmogenic ^{10}Be in 16 striated bedrock samples and 14 erratic boulders allow us to make inferences about subglacial erosion efficiency and deduce the pattern, timing, and rate of early Holocene ice margin retreat. After understanding these parameters for Sikuijuitsoq Fjord, we draw comparisons with the behavior of Jakobshavn Isbræ and show that the chronologies, rates, and dynamics of deglaciation are similar. Our goal is to determine if fast-flowing ice in Jakobshavn Isbræ exerted control on the neighboring ice margin and thus on the concentration of ^{10}Be in the samples we collected.

2. Study site and previous work

We collected samples near and along the narrow (~3 km) Sikuijuitsoq Fjord located on the western margin of the Greenland Ice Sheet. Just to the south is Jakobshavn Isbræ (Figs. 1 and 2; 50°W, 69°N), one of the largest outlet glaciers in the world. At present, the calving margin of Jakobshavn Isbræ is about 50 km east of the town of Ilulissat. The outlet glacier drains through Jakobshavn Isfjord, which is 6–8 km wide, up to 1000 m deep (Holland et al., 2008), and almost entirely choked with icebergs due to a shallow shoal at the fjord mouth. Both fjords have inclined rather than vertical walls and the surrounding topography reaches almost 700 m a.s.l. The ice-free landscape between the coast of Disko Bugt and the present ice margin contains glacially-scoured bedrock and ubiquitous erratic boulders, which lie both on moraines and directly on bare bedrock surfaces (Fig. 3).

The prominent Fjord Stade moraines (Fig. 2), which lie between Disko Bugt and the present-day ice margin, were deposited during the early Holocene; these moraines consist of the sometimes overlapping outer “Marrait” and inner “Tasiussaq” moraines (Weidick, 1968; Weidick and Bennike, 2007; Young et al., 2011). The Marrait and Tasiussaq moraines form a single complex, which allows the landscape to be divided into two chronologically-distinct land surfaces: an older surface outside of the moraines and a younger surface inside of the moraines.

2.1. Outer land surface

The land surface outside of the Fjord Stade moraine complex contains the oldest terrain surrounding Jakobshavn Isfjord (Fig. 2). During the last glaciation, ice extended across Disko Bugt and onto the continental shelf (Weidick and Bennike, 2007). Radiocarbon ages from marine sediment cores suggest that deglaciation through

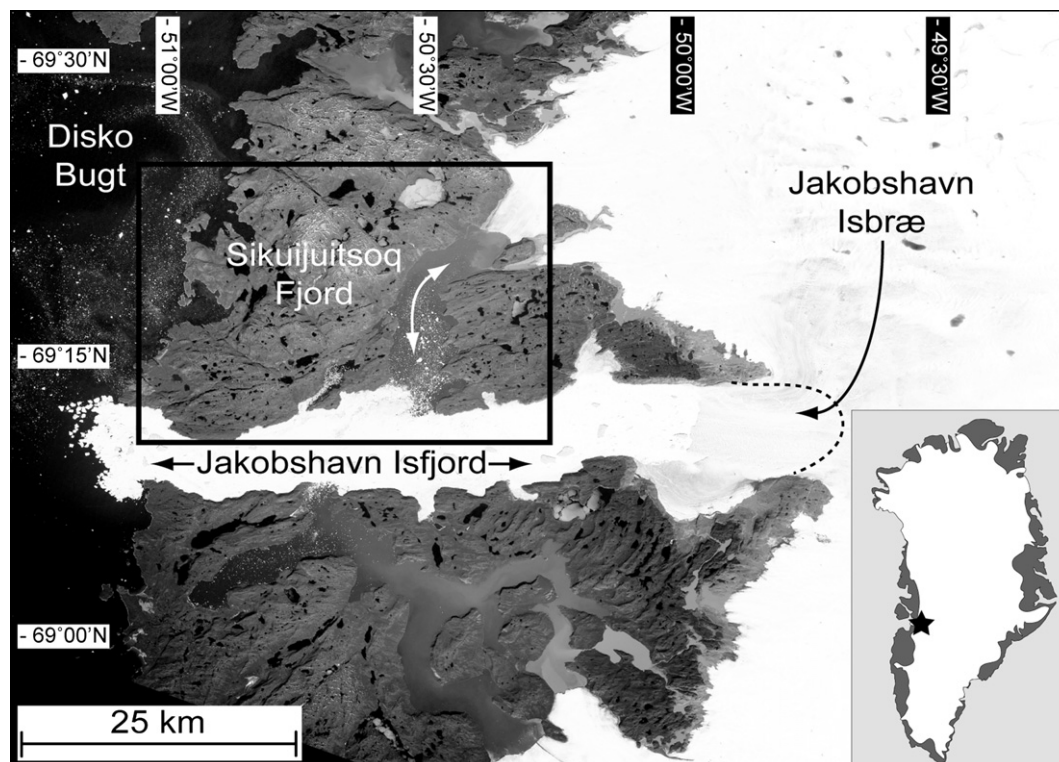


Fig. 1. Sikuijuitsoq Fjord is a northerly tributary of Jakobshavn Isfjord, located on the western margin of the Greenland Ice Sheet. Inset: Location of study area is shown by the star. Main image: Aerial imagery of Sikuijuitsoq Fjord, Jakobshavn Isfjord, and Jakobshavn Isbræ. The box indicates the area covered by Fig. 2, and the black dashed line shows the approximate modern location of the calving margin of Jakobshavn Isbræ (Csatho et al., 2008). Image courtesy of NASA Landsat Program (2001).

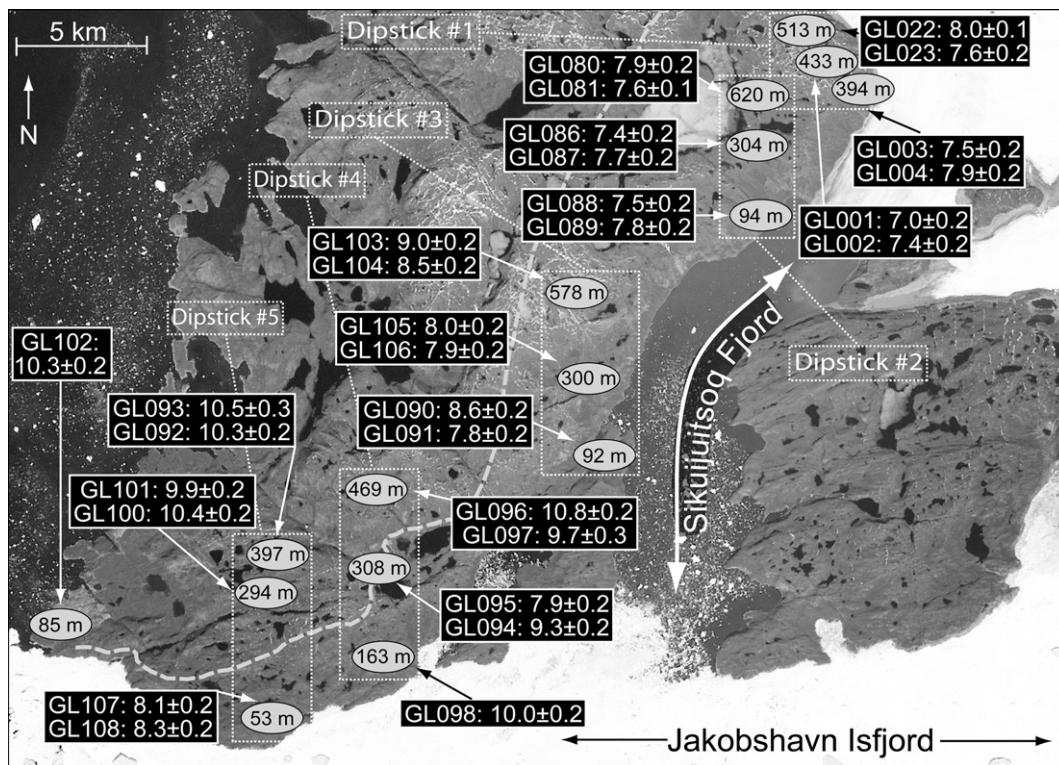


Fig. 2. Bedrock and boulder samples were collected along a 40-km transect north of Jakobshavn Isfjord, parallel to the northern tributary Sikujuitsoq Fjord. Wherever possible, bedrock/boulder pairs were taken from high, medium, and low elevations shown by gray ovals. At each sampling location, model ^{10}Be ages are shown (expressed in ka, with 1σ internal error), with the bedrock sample listed first and the boulder sample listed second; in the two instances where boulders were not available, only the bedrock ^{10}Be ages are listed. The gray dashed line shows the approximate location of the Fjord Stade moraine complex. Image courtesy of NASA Landsat Program (2001).

Disko Bugt took place at or prior to ~ 10.3 cal ka BP (Long and Roberts, 2003; Lloyd et al., 2005); this represents a maximum limiting age for the outer land surface. Radiocarbon ages from raised marine deposits on this surface provide a minimum estimate

of deglaciation at $\sim 9.9 \pm 0.1$ cal ka BP ($n = 4$) (Weidick and Bennike, 2007). More recently, ^{10}Be surface exposure ages suggest that this surface is $\sim 10.2 \pm 0.1$ ka ($n = 5$) (Young et al., 2011). The body of previous work discussed above constrains the age of the



Fig. 3. The land surface surrounding Sikujuitsoq Fjord is characterized by striated, sculpted bedrock outcrops and ubiquitous erratic boulders. There is negligible till cover. Here, a sample (GL091) is collected from a large boulder lying directly on ice-sculpted bedrock.

outer land surface to ~10 ka, and serves as a maximum limiting age for the Fjord Stade moraine complex.

2.2. Inner land surface

The land surface inside of the Fjord Stade moraine complex was deglaciated after the abandonment of the Tasiussaq moraine and contains the youngest terrain outside of the historic moraine immediately adjacent to today's ice margin (Fig. 2). Basal radiocarbon ages from a lake sediment core southeast of Disko Bugt suggest a minimum limiting age of ~8.0–7.7 cal ka BP (Long and Roberts, 2002); similarly, basal radiocarbon measurements from two lakes above the marine limit just south of Jakobshavn Isfjord provide minimum limiting ages of ~7.7 and 7.6 cal ka BP (Long et al., 2006). More recently, ^{10}Be surface exposure ages constrain the age of the inner land surface to 8.0 ± 0.1 ka ($n = 5$), not including an older outlier of 12.0 ± 0.3 ka (Young et al., 2011). The work discussed above demonstrates that this surface was deglaciated ~8 ka, thereby providing a minimum limiting age for the Fjord Stade moraine complex.

The inner land surface spans the distance from the Fjord Stade moraine complex to the historic moraine. Therefore, the exposure age of this surface varies with distance from the ice sheet margin, reflecting the rate of ice margin retreat. Additional ^{10}Be surface exposure ages from directly outside of the historic moraine near Jakobshavn Isbræ suggest that the ice margin at Jakobshavn Isfjord reached its present position $\sim 7.5 \pm 0.2$ ka ($n = 7$) (Young et al., 2011), or about 0.5 ka after the abandonment of the Tasiussaq moraines. Similarly, basal radiocarbon ages from lake sediment cores show that the ice margin first reached its present position ~7.4–7.2 cal ka BP (Briner et al., 2010). Radiocarbon ages ($n = 15$) of marine fauna reworked into the historic moraine range from 6.1 to 2.2 cal ka BP, indicating that the ice margin retreated behind its present-day position before 6.1 cal ka BP and re-advanced to its current position after 2.2 cal ka BP (Weidick et al., 1990; Weidick and Bennike, 2007).

3. Methods

3.1. Experimental design

We collected 16 bedrock and 14 boulder samples for the analysis of *in situ* cosmogenic ^{10}Be (Gosse and Phillips, 2001). Samples were collected along a 40-km southwest to northeast transect extending from Disko Bugt to the present-day ice margin, along Sikuijuitsoq Fjord, a tributary to Jakobshavn Isfjord (Table 1; Fig. 2). The sampling scheme used in this study, known as “dipstick sampling” (Stone et al., 2003), involves collecting bedrock and boulder pairs at a variety of elevations at several locations along a transect normal to the ice margin. Samples were collected at elevations ranging from 50 to 620 m a.s.l. and included high-, medium-, and low-elevation bedrock/boulder pairs at each “dipstick” wherever possible. This sampling scheme provides a three-dimensional pattern of exposure ages, yielding information about both the vertical and horizontal timing of ice retreat. Measuring ^{10}Be in paired bedrock and boulder samples provides information about the efficiency of subglacial erosion and the likelihood of post-depositional burial. If a bedrock sample is appreciably older than a paired boulder sample, inheritance of ^{10}Be from prior periods of exposure is likely (Bierman et al., 1999). If a bedrock sample is appreciably younger than a paired boulder sample, localized shielding by till or snow cover is possible. If the two ages agree, the likelihood of complex exposure histories is low, and both ages are more likely to be accurate.

The relationships among the sample dipsticks, the Fjord Stade moraines, and thus the inner and outer land surface vary by location. Since the fjord walls are sloped rather than vertical, sampled dipsticks span several km of horizontal distance in order to capture the full extent of local vertical relief. The two dipsticks closest to the coastline (numbers 5 and 4) have their low-elevation samples on the edge of Jakobshavn Isfjord, while the next three (numbers 3, 2, and 1) have their low-elevation samples on the edge of the Sikuijuitsoq tributary fjord. The two dipsticks closest to the coastline (numbers 5 and 4) span the Fjord Stade moraine complex; thus, their low-elevation samples are from the inner land surface, and their high-elevation samples are from the outer land surface. The three dipsticks closest to the present-day ice margin (numbers 3, 2, and 1) are entirely inboard of the Fjord Stade moraine complex.

3.2. Field methods

Using a chisel and hammer, we collected the top several cm of material from flat-lying, glacially-scoured bedrock surfaces and erratic boulders (Table 1). To avoid complex cosmic-ray exposure geometries, we did not collect samples from areas that were sheltered by steep hillsides, cliffs, or large boulders. Wherever possible, we sampled bedrock and boulder pairs in close proximity, usually less than 5 m apart. Latitude/longitude and elevation data were collected with a handheld Garmin 12 GPS that has a positional uncertainty of <10 m; elevation uncertainty is <25 m.

3.3. Quartz and beryllium isolation

Samples for ^{10}Be analysis were prepared using mineral separation procedures modified from Kohl and Nishiizumi (1992). Rocks were crushed, ground, and sieved to isolate grains between 250 and 850 μm , then magnetically separated to remove mafic minerals. Samples were ultrasonically etched twice in hot 6N HCl to remove grain coatings, and then three more times in hot, dilute (1%) HF-HNO₃ to preferentially dissolve all grains except quartz. If needed, we performed a heavy-liquid density separation. Quartz was tested for purity by inductively coupled plasma optical emission spectrometry, and subsequent HF-HNO₃ etches were performed until desired purity levels were reached (usually less than 100 ppm Al and less than 200 ppm total cations).

Beryllium was isolated in the University of Vermont Cosmogenic Laboratory (see www.uvm.edu/cosmolab, Table 1). For each sample, between ~5 and 20 g of purified quartz was used for analysis. Samples were prepared in batches of 12, including either 1 or 2 process blanks. Just over 1 g of low-level ^9Be carrier (245 ppm concentration) made from beryl at the University of Vermont was added to each sample, equating to an addition of ~250 μg of ^9Be . Complete dissolution took place with 100 g of hot, concentrated HF. After dissolution and drydown, samples were treated with four additions of HClO₄, and then converted to chloride form with two additions of HCl. Samples were passed through anion exchange columns to remove Fe, converted to sulfate form with two additions of H₂SO₄, and passed through cation exchange columns primarily to separate Ti, Be, and Al, and to remove B. Average Be recovery for these samples was $96.2 \pm 5.7\%$ (1σ , $n = 30$). The Be fraction was precipitated at pH 8 as hydroxide gel, dried, ignited to produce BeO, and packed into stainless steel cathodes with Nb powder at a 1:1 M ratio for accelerator mass spectrometry (AMS) measurements.

3.4. Isotopic analysis

$^{10}\text{Be}/^9\text{Be}$ ratios were measured by AMS at Lawrence Livermore National Laboratory. All samples were normalized to standard 07KNSTD3110, with a reported ratio of $2850 \cdot 10^{-15}$ (Nishiizumi

Table 1
Sample collection and laboratory information for 16 bedrock samples and 14 boulder samples at Sikujuitsoq Fjord. Samples were collected in six “dipsticks” at a range of elevations along a 40-km transect normal to the ice margin.

Sample name	Sample type	Dipstick number	Land surface	Elevation (m)	Latitude (°N) ^a	Longitude (°E) ^a	Thickness (cm)	Quartz (g)	⁹ Be (μg) ^b	¹⁰ Be/ ⁹ Be Ratio ^c	Uncertainty ^d	¹⁰ Be Conc (atoms/g) ^e	Exposure age (ka) ^e	Uncertainty (ka) ^d
GL022	Bedrock	1	Inner	515	69.432	-50.289	5	20.60	247	6.90 × 10 ⁻¹⁴	1.28 × 10 ⁻¹⁵	5.54 × 10 ⁴	8.0	0.1
GL023	Boulder	1	Inner	511	69.433	-50.289	3	19.86	248	6.41 × 10 ⁻¹⁴	1.41 × 10 ⁻¹⁵	5.35 × 10 ⁴	7.6	0.2
GL001	Bedrock	1	Inner	434	69.433	-50.272	1	19.39	247	5.43 × 10 ⁻¹⁴	1.58 × 10 ⁻¹⁵	4.62 × 10 ⁴	6.9	0.2
GL002	Boulder	1	Inner	432	69.433	-50.273	2	19.90	247	5.85 × 10 ⁻¹⁴	1.37 × 10 ⁻¹⁵	4.86 × 10 ⁴	7.4	0.2
GL003	Bedrock	1	Inner	395	69.434	-50.266	3	19.86	248	5.67 × 10 ⁻¹⁴	1.43 × 10 ⁻¹⁵	4.73 × 10 ⁴	7.5	0.2
GL004	Boulder	1	Inner	392	69.434	-50.266	2	20.46	248	6.16 × 10 ⁻¹⁴	1.47 × 10 ⁻¹⁵	4.99 × 10 ⁴	7.9	0.2
GL080	Bedrock	2	Inner	621	69.395	-50.416	3	17.58	247	6.58 × 10 ⁻¹⁴	1.47 × 10 ⁻¹⁵	6.18 × 10 ⁴	7.9	0.2
GL081	Boulder	2	Inner	618	69.395	-50.416	1.5	18.96	247	6.90 × 10 ⁻¹⁴	1.30 × 10 ⁻¹⁵	6.01 × 10 ⁴	7.6	0.1
GL086	Bedrock	2	Inner	304	69.374	-50.458	2.5	20.26	247	5.26 × 10 ⁻¹⁴	1.35 × 10 ⁻¹⁵	4.28 × 10 ⁴	7.4	0.2
GL087	Boulder	2	Inner	303	69.374	-50.458	2	19.99	248	5.38 × 10 ⁻¹⁴	1.16 × 10 ⁻¹⁵	4.45 × 10 ⁴	7.7	0.2
GL088	Bedrock	2	Inner	95	69.344	-50.429	2.5	16.59	249	4.38 × 10 ⁻¹⁴	1.05 × 10 ⁻¹⁵	3.49 × 10 ⁴	7.5	0.2
GL089	Boulder	2	Inner	93	69.344	-50.429	2.5	19.22	247	4.20 × 10 ⁻¹⁴	9.41 × 10 ⁻¹⁶	3.61 × 10 ⁴	7.8	0.2
GL103	Bedrock	3	Inner	578	69.318	-50.640	1	19.63	247	8.19 × 10 ⁻¹⁴	2.04 × 10 ⁻¹⁵	6.89 × 10 ⁴	9.0	0.2
GL104	Boulder	3	Inner	578	69.318	-50.640	5	19.89	247	7.54 × 10 ⁻¹⁴	1.44 × 10 ⁻¹⁵	6.26 × 10 ⁴	8.5	0.2
GL105	Bedrock	3	Inner	300	69.293	-50.602	1	17.00	246	4.81 × 10 ⁻¹⁴	1.11 × 10 ⁻¹⁵	4.65 × 10 ⁴	8.0	0.2
GL106	Boulder	3	Inner	300	69.293	-50.602	2	20.63	247	5.71 × 10 ⁻¹⁴	1.18 × 10 ⁻¹⁵	4.58 × 10 ⁴	7.9	0.2
GL090	Bedrock	3	Inner	93	69.269	-50.581	2	20.64	252	4.92 × 10 ⁻¹⁴	1.03 × 10 ⁻¹⁵	4.02 × 10 ⁴	8.6	0.2
GL091	Boulder	3	Inner	91	69.269	-50.582	2	10.65	248	2.32 × 10 ⁻¹⁴	6.41 × 10 ⁻¹⁶	3.61 × 10 ⁴	7.8	0.2
GL096	Bedrock	4	Outer	468	69.250	-50.823	3	15.28	247	6.72 × 10 ⁻¹⁴	1.29 × 10 ⁻¹⁵	7.27 × 10 ⁴	10.8	0.2
GL097	Boulder	4	Outer	470	69.251	-50.822	2	16.35	247	6.54 × 10 ⁻¹⁴	1.70 × 10 ⁻¹⁵	6.62 × 10 ⁴	9.7	0.3
GL094	Boulder	4	N/A ^f	308	69.229	-50.810	1	13.33	247	4.43 × 10 ⁻¹⁴	1.16 × 10 ⁻¹⁵	5.49 × 10 ⁴	9.3	0.2
GL095	Bedrock	4	N/A ^f	308	69.229	-50.810	2.5	21.49	247	6.00 × 10 ⁻¹⁴	1.68 × 10 ⁻¹⁵	4.61 × 10 ⁴	7.9	0.2
GL098	Bedrock	4	Inner	163	69.199	-50.791	3	16.76	248	5.04 × 10 ⁻¹⁴	1.08 × 10 ⁻¹⁵	4.97 × 10 ⁴	10.0	0.2
GL092	Boulder	5	Outer	397	69.230	-50.902	1	20.14	248	8.01 × 10 ⁻¹⁴	1.59 × 10 ⁻¹⁵	6.59 × 10 ⁴	10.3	0.2
GL093	Bedrock	5	Outer	397	69.230	-50.902	2	18.94	246	7.71 × 10 ⁻¹⁴	1.94 × 10 ⁻¹⁵	6.69 × 10 ⁴	10.5	0.3
GL100	Boulder	5	Outer	292	69.227	-50.930	2	15.53	247	5.60 × 10 ⁻¹⁴	1.22 × 10 ⁻¹⁵	5.95 × 10 ⁴	10.4	0.2
GL101	Bedrock	5	Outer	295	69.227	-50.929	3.5	20.19	247	6.87 × 10 ⁻¹⁴	1.30 × 10 ⁻¹⁵	5.62 × 10 ⁴	9.9	0.2
GL107	Bedrock	5	Inner	53	69.180	-50.891	1	20.68	248	4.57 × 10 ⁻¹⁴	1.01 × 10 ⁻¹⁵	3.66 × 10 ⁴	8.1	0.2
GL108	Boulder	5	Inner	53	69.180	-50.891	1	15.14	249	3.39 × 10 ⁻¹⁴	9.32 × 10 ⁻¹⁶	3.73 × 10 ⁴	8.3	0.2
GL102	Bedrock	6	Outer	85	69.207	-51.134	1	19.65	247	5.70 × 10 ⁻¹⁴	1.27 × 10 ⁻¹⁵	4.79 × 10 ⁴	10.3	0.2

^a Locations and elevations were recorded in the field with a Garmin GPS-12.

^b Samples were prepared with a low-level beryllium carrier of 245 ppm concentration.

^c Ratios were measured at the Lawrence Livermore National Laboratory and were normalized to the standard 07KNSD3110 (Nishiizumi et al., 2007). Reported ratios have already been blank-corrected (the blank ratios ranged from 4.4 × 10⁻¹⁶ to 1.0 × 10⁻¹⁵, or 1–3% of the samples).

^d Reported uncertainties are internal AMS uncertainties.

^e Ages were calculated using the northeastern North American production rate and the Lal (1991)/Stone (2000) scaling scheme in the CRONUS Earth online calculator. Ages have been scaled for elevation, sample density, sample thickness, latitude, and longitude.

^f This sample pair was collected in between the two Fjord Stade moraines, on neither the inner nor the outer land surface.

et al., 2007). Measured sample ratios ranged from $2.3 \cdot 10^{-14}$ to $8.2 \cdot 10^{-14}$, and AMS measurement precisions, including propagated blank corrections, ranged from 1.9 to 3.0% (1σ , Table 1). Samples were prepared in three separate batches, and the process blanks for these three batches contained $1.7 \cdot 10^4$ ($n = 1$), $7.3 \cdot 10^3$ (average, $n = 2$), and $1.5 \cdot 10^4$ ($n = 1$) ^{10}Be atoms, respectively. The blank $^{10}\text{Be}/^9\text{Be}$ ratios were $1.0 \cdot 10^{-15}$ ($n = 1$), $4.4 \cdot 10^{-16}$ (average, $n = 2$), and $9.3 \cdot 10^{-16}$ ($n = 1$); these blanks were inconsequential as they amounted to only 1–3% of the total sample ratios.

3.5. Exposure age calculations

^{10}Be exposure ages were calculated with the CRONUS Earth online exposure age calculator developmental version 2.2, constants version 2.2 (Balco et al., 2008). We used the regionally-calibrated northeastern North American production rate of 3.93 ± 0.19 atoms $\text{g}^{-1} \text{yr}^{-1}$ (Balco et al., 2009) and the Lal/Stone constant production rate model and scaling scheme (Lal, 1991; Stone, 2000) under standard atmosphere. We chose to use the northeastern North American production rate because ^{10}Be ages calculated this way correlated closely with the independent chronology deduced from other dating methods (e.g. radiocarbon; Section 2). Calculated ^{10}Be ages can vary by as much as 14% based on the chosen production rate, and as much as 4% based on the chosen scaling scheme. In CRONUS, corrections were made for latitude, elevation, sample thickness (ranged from 1 to 5 cm), and sample density (2.7 g cm^{-3} ; Table 1).

No corrections were made for snow cover. Shielding by snow cover would lead to ^{10}Be age underestimates (Schildgen et al., 2005); however, snow cover effects at our sample sites are likely minimal. Using contemporary data from a weather station on the southern side of Disko Bugt (www.weather-and-climate.com, Egedesminde station), we determined that mean temperatures are below freezing for eight months of the year (October through May) and that ~ 180 mm of snow (water equivalent) falls during this time at a rate of ~ 15 – 30 mm per month. To assess the significance of potential snow shielding, we assumed that precipitation was added in monthly increments, and that no melting or sublimation occurred until May. Shielding calculated according to Gosse and Phillips (2001) suggests that reported exposure ages could underestimate the true age by no more than 7%. This calculation is likely a significant overestimate because we did not account for snow loss during the winter and because the areas we sampled are likely windswept and exposed during winter months. However, this calculation was performed with only modern snowfall data; if snowfall was different over the course of the Holocene, shielding values may have been lesser or greater than modern data suggest.

No corrections were made for erosion, till cover, or isostatic rebound. Bedrock and boulder erosion can also cause ^{10}Be concentrations to underestimate exposure ages; however, all of the outcrops and boulders we sampled had fresh surfaces and some preserved striations, leading us to conclude that erosion of rock during the Holocene was negligible. The field area contains little till; boulders lie directly on bare bedrock surfaces. Thus, we consider shielding by now-eroded till unlikely. We did not correct sample elevations for post-glacial isostatic rebound because corrections calculated by Young et al. (2011) in the same area all fall within our vertical GPS uncertainty, and amount to less than 1–2% of calculated exposure ages.

Reported age uncertainties reflect AMS errors only, which we refer to as “internal”. We use internal uncertainties in our data analysis because we are interested in how the sample ages within this data set relate to each other. This approach allows us to investigate relationships between samples, e.g. testing for inheritance with paired bedrock and boulder samples. We acknowledge

that there are additional age uncertainties related to production rate calibration as well as elevation and latitude scaling that would reflect better the precision of our ages when making comparison to other dating methods and cosmogenic ages from other locations. However, because our samples come from a geographically limited region and a restricted elevation range, errors in calibration and correction are correlated and thus affect all samples similarly.

4. Results

All 30 cosmogenic ^{10}Be exposure ages are indicative of Holocene exposure. Bedrock and boulder samples had measured ^{10}Be concentrations of $7.3 \cdot 10^4$ – $3.5 \cdot 10^4$ atoms g^{-1} , yielding ^{10}Be ages of 10.8 ± 0.2 – 6.9 ± 0.2 ka ($n = 30$; Table 1 & Fig. 2). Corresponding bedrock and boulder sample pairs have similar ^{10}Be ages ($r^2 = 0.72$, Fig. 4); a repeated measures t -test verifies that there is no statistically significant difference when boulders and bedrock ages are considered in a paired comparison ($p = 0.980$). Similarly, considering bedrock and boulder samples in two distinct populations results in nearly identical population distributions (Fig. 5); an

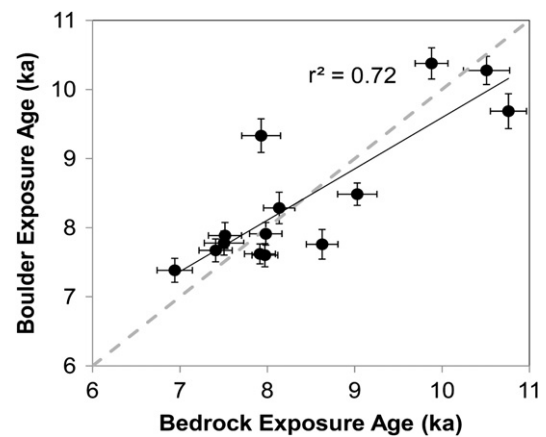


Fig. 4. Bedrock and boulder ages at sample sites are correlated with a slope of 0.74 ($r^2 = 0.72$). The dashed gray line represents a 1:1 ratio between bedrock and boulder sample ages, and the solid line is the linear regression. Error bars show 1σ internal error.

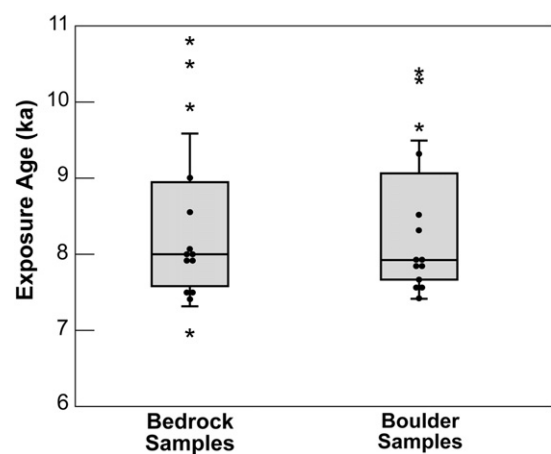


Fig. 5. Box and whisker plots of bedrock and boulder age populations. The box encloses the area between the first and third quartiles, and the horizontal line represents the median. Whiskers show one standard deviation. Samples that lie outside one standard deviation from the mean are shown with an asterisk; all other samples are shown with dots.

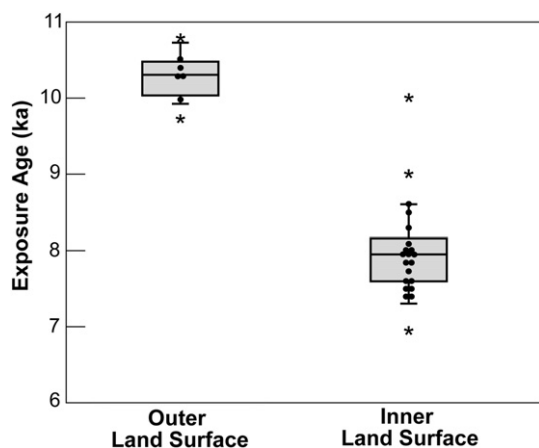


Fig. 6. Box and whisker plots of sample age populations from the land surfaces outside and inside of the Fjord Stade moraine complex. The box encloses the area between the first and third quartiles, and the horizontal line represents the median. Whiskers show one standard deviation. Samples that lie outside one standard deviation from the mean are shown with an asterisk; all other samples are shown with dots.

independent samples *t*-test indicates that there is no statistical difference between populations ($p = 0.973$).

Eleven of the 14 bedrock/boulder pairs have indistinguishable ^{10}Be ages; only three of the 14 pairs have ^{10}Be ages that differ by more than the 1σ AMS uncertainties. In one of these cases, the boulder sample (GL094, 9.3 ± 0.2 ka) is older than the bedrock sample (GL095, 7.9 ± 0.2 ka) by 1.4 ka (3σ). One low-elevation bedrock sample (GL090, 8.6 ± 0.2 ka) is 0.8 ka (2σ) older than its corresponding boulder (GL091, 7.8 ± 0.2 ka), and one high-elevation bedrock sample (GL096, 10.8 ± 0.2 ka) is 1.1 ka (2σ) older than its corresponding boulder sample (GL097, 9.7 ± 0.3 ka). The reason for bedrock/boulder discordance in these three sample pairs is unknown.

Sample ^{10}Be ages differ according to the location on the landscape where the samples were collected (Fig. 6). Samples from the land surface outside of the Fjord Stade moraine complex have an average age of 10.3 ± 0.4 ka ($n = 7$). Samples from the land surface inside of the Fjord Stade moraine complex have an average age of 8.0 ± 0.7 ka ($n = 21$). An independent samples *t*-test indicates that these are separable populations ($p < 0.001$).

There is a scatter of ^{10}Be ages within each dipstick (Fig. 7). There is more scatter in the two outboard dipsticks (numbers 5 and 4), which span the Fjord Stade moraines (relative standard deviations = 11.3 and 10.9%). The three dipsticks closest to the present-day ice margin (numbers 3, 2, and 1) are entirely inboard of the Fjord Stade moraine complex and have less scatter (relative standard deviations = 6.0, 2.4, and 4.9%). Within these three inner dipsticks, there is no significant difference between high-, middle-, and low-elevation samples at 1σ . However, sample ^{10}Be ages decrease towards the present-day ice margin (Figs. 7 and 8); the average ages (1σ) of dipstick numbers 3, 2, and 1 are 8.3 ± 0.5 ka ($n = 6$), 7.7 ± 0.2 ka ($n = 6$), and 7.6 ± 0.4 ka ($n = 6$). A one-way ANOVA shows that the ages of these three dipsticks are separable ($p = 0.006$, Fig. 8). Subsequent independent samples *t*-tests show that the age of dipstick 3 is separable from both the age of dipstick 1 ($p = 0.014$) and the age of dipstick 2 ($p = 0.011$), but the age of dipstick 1 is not separable from the age of dipstick 2 ($p = 0.591$).

5. Discussion

Cosmogenic analysis of paired bedrock/boulder samples provides a powerful means by which to understand the dynamics

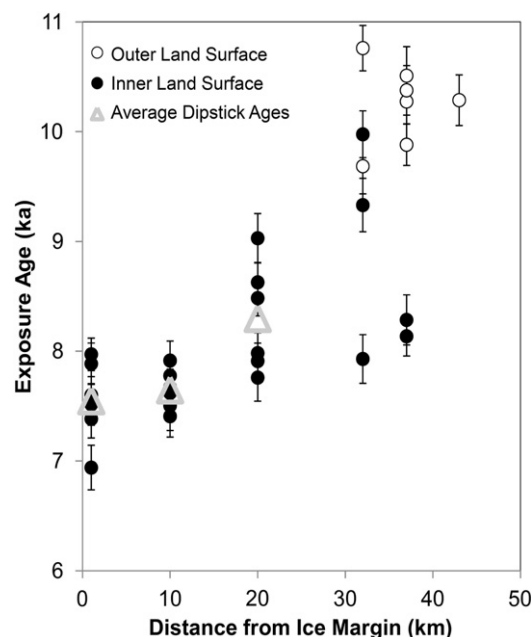


Fig. 7. ^{10}Be ages of bedrock and boulder samples plotted against distance from the present-day ice sheet margin. Bars show 1σ internal error. Sample ^{10}Be ages show an overall decreasing trend towards the present-day ice sheet margin. Average dipstick ages have been calculated for the three inner-most dipsticks, which do not crosscut the Fjord Stade moraine complex.

of bedrock erosion by ice, improve the accuracy of deglaciation chronologies, estimate rates of ice retreat, and test the influence of large ice streams on adjacent but less dynamic ice margins.

5.1. Cosmogenic nuclide inheritance and last glaciation erosion rates

The Holocene ages of all samples from Sikujitsoq Fjord and the robust correlation of paired bedrock and boulder ages (Figs. 4 and 5) both argue that inheritance of cosmogenic nuclides from exposure before the last glaciation is unlikely in this field area. Such exposure could have occurred during the Eemian period when ice

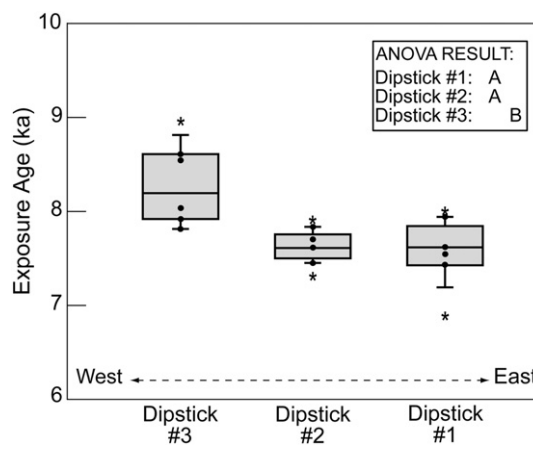


Fig. 8. Box and whisker plots of sample age populations from the three eastern-most dipsticks, which do not crosscut the Fjord Stade moraine complex. The box encloses the area between the first and third quartiles, and the horizontal line represents the median. Whiskers show one standard deviation. Samples that lie outside one standard deviation from the mean are shown with an asterisk; all other samples are shown with dots. ANOVA results are shown in the upper right.

extent was much reduced (Létréguilly et al., 1991; Cuffey and Marshall, 2000; Otto-Bliesner et al., 2006), and during many previous interglaciations throughout the Quaternary when global ice volume was low (Lisiecki and Raymo, 2005). The observed lack of inheritance indicates that glacial ice near Ilulissat was highly erosive during the last glaciation, likely removing at least ~ 2 m of material from bedrock outcrops. Our results are consistent with the abundance of fresh-appearing glacially-scoured bedrock at all elevations visited in the field (Roberts and Long, 2005).

This result differs notably from findings in some other high-latitude areas, where subglacial erosion rates are insufficient to remove ^{10}Be inherited from previous periods of exposure. In these cases, bedrock samples have old exposure ages even though they were overruled by ice during the last glaciation. Such inheritance has been documented in Greenland (Håkansson et al., 2008; Kelly et al., 2008; Corbett et al., 2009), the Canadian Arctic (Bierman et al., 1999; Briner et al., 2003; Marquette et al., 2004), Scandinavia (Stroeven et al., 2002; Harbor et al., 2006), and Antarctica (Sugden et al., 2005; Lilly et al., 2010). The lack of inheritance around Sikujuitsoq Fjord is likely due to the presence of thick, fast-flowing ice surrounding Jakobshavn Isbræ, creating an ideal environment for the removal of previously exposed bedrock and boulders (Bougamont and Tulaczyk, 2003; Roberts and Long, 2005; Smith et al., 2007). These results suggest that bedrock and boulder samples adjacent to large ice streams are less likely than samples from other geomorphic settings to contain inherited nuclides. In settings such as this, both sculpted bedrock and erratic boulders provide similarly accurate deglaciation chronologies.

5.2. Comparison to existing land surface chronology

Data from Sikujuitsoq Fjord agree well with previous estimates of land surface age and confirm the existence of two chronologically-distinct land surfaces (Fig. 6). Samples collected from the land surface outside of the Fjord Stade moraine complex provide an average ^{10}Be age of 10.3 ± 0.4 ka ($n = 7$). This age is in close agreement with previous limiting age constraints discussed in Section 2.1, and is indistinguishable from the ^{10}Be age of $\sim 10.2 \pm 0.1$ ka ($n = 5$) from Young et al. (2011).

Samples from the land surface inside of the Fjord Stade moraine complex provide an average ^{10}Be age of 8.0 ± 0.7 ka ($n = 21$), integrated over a wide geographic area. Samples from directly inside the moraine complex give an average age of 8.2 ± 0.1 ka ($n = 2$), in close agreement with previous work from Jakobshavn Isfjord discussed above (Young et al., 2011), and provide a minimum limiting age for abandonment of the Tasiussaq moraine. Some of the samples from this land surface were collected from directly outside the historic moraine, and provide an average ^{10}Be age of 7.6 ± 0.4 ka ($n = 6$). These samples provide an estimate of when the ice margin near Sikujuitsoq Fjord retreated behind the position of the historic moraine, and are again in close agreement with previous findings (7.5 ± 0.2 ka, $n = 7$) for samples from the same landscape position but in Jakobshavn Isfjord (Young et al., 2011).

Two samples from the inner land surface have older-than-expected ^{10}Be ages. Previous work suggests that the inner (Tasiussaq) moraine was deposited ~ 8.2 ka (Long and Roberts, 2002; Weidick and Bennike, 2007; Young et al., 2011), consistent with the average age we measure for the inner land surface 8.0 ± 0.7 ka ($n = 21$). However, two bedrock samples (GL098 and GL103) from just inboard of the Fjord Stade moraine are more than 1σ above the average. Bedrock sample GL098 (10.0 ± 0.2 ka) is indistinguishable from the age of the outer land surface (~ 10 ka, Fig. 6). Bedrock sample GL103 (9.0 ± 0.2 ka) is 500 years older than its paired boulder and 1000 years older than the average age of the inner land surface. These differences are best explained by

inheritance of nuclides resulting from early Holocene exposure. The ice margin retreated inboard of the GL098 and GL103 sample locations ~ 10 ka, exposing the entire outer land surface and some of the more distal portions of the inner land surface. Then, the ice re-advanced and deposited the Fjord Stade moraine complex; however, this re-advance was too short-lived to completely remove ^{10}Be formed in outcrops near the moraine after the 10 ka retreat and before the 8.2 ka advance. Although this inheritance is only shown by two samples, these data hint that bedrock samples collected just inboard of moraines created by short-lived re-advances may be more likely to carry inherited nuclides and could therefore overestimate actual exposure ages. In cases like this, paired bedrock/boulder samples are particularly useful.

5.3. Ice surface lowering

There is no difference in sample ^{10}Be age with elevation (within 1σ uncertainties) at the three dipsticks contained within the inner land surface. This differs from other high-latitude studies, which have documented measurable ice downwasting rates in both Greenland and Antarctica. Ice surface lowering rates in the early Holocene were ~ 6 cm yr^{-1} near Sisimiut Fjord, western Greenland (Rinterknecht et al., 2009), and ~ 2.5 – 9 cm yr^{-1} in Marie Byrd Land, Antarctica (Stone et al., 2003). The lack of a measurable downwasting rate does not imply that ice surface lowering did not occur; rather, the data suggest that any vertical change in ice position at each dipstick took place more rapidly than the resolution of the ^{10}Be chronometer, probably within several decades to at most a few centuries. The rapid change in ice thickness we infer for deglaciation near Sikujuitsoq Fjord may be unique to areas with marine-terminating glaciers. Given that the glacier in Sikujuitsoq Fjord was predominately marine-terminating, the ice margin was likely near-vertical, as seen at other calving fronts. This steep geometry would have exposed each dipstick more rapidly than a lower-slope margin more characteristic of terrestrial ice fronts.

5.4. Lateral ice margin retreat

Ice margin retreat through Sikujuitsoq Fjord occurred rapidly after the abandonment of the inner Fjord Stade moraine. Abundant previous work demonstrates that the Tasiussaq moraine was deposited during a re-advance ~ 8.2 ka (Section 2.2), and Young et al. (2011) suggest that the ice margin left the moraine ~ 8.0 ka ($n = 5$). The ice margin went behind the position of the historic moraine only ~ 400 years later (~ 7.6 ka, $n = 6$, this study), after retreating 40–45 km.

Since it is unclear when ice flow separation between the two fjords occurred, we cannot determine whether the direction of ice flow was regionally controlled (by the presence of a large ice stream flowing through Jakobshavn Isfjord) or locally controlled (by the orientation of Sikujuitsoq Fjord). Therefore, we calculate ice margin retreat rates in two ways: assuming that ice retreat was west to east, parallel to Jakobshavn Isfjord (a distance of ~ 40 km), and assuming that ice retreat was southwest to northeast, parallel to Sikujuitsoq Fjord (a distance of ~ 45 km). Assuming that retreat began after the abandonment of the Tasiussaq moraine at 8.0 ka, and ended when the ice margin retreated behind the historic moraine at 7.6 ka, we calculate integrated retreat rates of ~ 100 and ~ 110 m yr^{-1} .

5.5. Sikujuitsoq Fjord and Jakobshavn Isfjord: deglaciation dynamics

The deglaciation chronologies at Sikujuitsoq Fjord and Jakobshavn Isfjord match closely (Section 5.2), most likely because the

two fjords were not separated for most of the early Holocene. The height of land that divides the two fjords has a maximum elevation of ~ 300 m. The inner land surface to the north of Sikujuitsoq Fjord extends to a much higher elevation (~ 500 – 600 m), as shown by the highest-elevation samples in dipstick numbers 1–3, which are still inboard of the Fjord Stade moraine complex. This relationship implies that, at the time of deposition of the inner Fjord Stade moraine, the two fjords had not yet become divided at the surface. Up until this point, and for a short time after, they both would have fed into a single outlet glacier. During retreat from the Fjord Stade moraines to the location of the historic moraine, the ice surface downwasted; rapid ice flow would have continued to occur in the fjords, but the flow over the dividing land surface would have slowed and eventually stagnated. The ice stream then must have separated into two distinct tongues; however, with retreat through this area lasting only 400 years, this configuration was not long-lived.

It is possible the retreat of Jakobshavn Isbræ through the main fjord set the pace for retreat of the ice margin in Sikujuitsoq Fjord. Initially, Jakobshavn Isfjord was filled with glacial ice, preventing sea water from coming in contact with the ice margin in Sikujuitsoq Fjord. However, as the grounding line progressed up Jakobshavn Isfjord and past the intersection with the tributary, sea water would have entered the mouth of Sikujuitsoq Fjord, causing the ice margin to float. This conversion to a marine-based ice margin may have initiated fast retreat in Sikujuitsoq Fjord, which continued at least until the margin reached its present-day position.

The data from this study imply that a major reorganization of Jakobshavn Isbræ ice flow occurred over a very short time period in the early Holocene. Between the time of deposition of the inner Fjord Stade moraine and the time when the ice retreated behind the position of the historic moraine, the vertical and horizontal extent of ice changed significantly. The ice margin retreated several tens of km horizontally at rates of ~ 100 m yr⁻¹, and lowered at rates too rapid to be measured using ¹⁰Be. During this period, the retreating margin exposed two distinct fjords, each containing tongues of ice that flowed independently as they do today.

5.6. Paleoclimatic context

Retreat of the ice margin at Sikujuitsoq Fjord was likely driven by external climate forcing and occurred simultaneously with ice retreat elsewhere in Greenland and around the world. Retreat of the ice margin through Disko Bugt and onto land ~ 10.3 – 10.2 ka coincided with rising mean annual temperatures in central Greenland (Dahl-Jensen et al., 1998; Vinther et al., 2009). Summer temperatures may have been as much as 5 °C warmer than today on Baffin Island (Axford et al., 2009). ¹⁰Be ages inboard of the Fjord Stade moraine complex constrain the deposition of the moraines to before 8.2 ± 0.1 ka. Although the age constraint is a minimum, it is likely a close constraint on deposition of the inner (Tasiussaq) Fjord Stade moraine (Young et al., 2011), and suggests that the Tasiussaq moraine in this region may represent a response of the ice sheet margin to the 8.2 ka event (Alley et al., 1997; Young et al., 2011). Retreat of the Sikujuitsoq ice margin between ~ 8.2 and ~ 7.6 ka to a location behind the historic moraine corresponded to increasing regional temperatures inferred from boreholes at the GRIP and DYE-3 ice core sites (Dahl-Jensen et al., 1998). A local temperature reconstruction depicts summers that were 2 °C warmer than modern between ~ 6 and 4.5 cal yr BP (Young et al., 2011), indicating that ice cover was substantially more reduced than today during this time period (Weidick et al., 1990). The ¹⁰Be ages presented in this study and in Young et al. (2011) demonstrate that the Sikujuitsoq and Jakobshavn ice margins retreated from the

Tasiussaq moraine, through their fjords, and behind the historic moraine in unison. This synchronicity suggests a common climatic forcing mechanism that dictated ice margin fluctuations in the Jakobshavn region during the Holocene.

5.7. Ice margin retreat rate comparisons

The rate of ice margin retreat (~ 100 m yr⁻¹) at Sikujuitsoq Fjord (after the abandonment of the Tasiussaq moraine at 8.0 ka, and before the ice margin retreated behind the historic moraine ~ 7.6 ka) is similar to other estimated retreat rates in the area for the same time period. At ~ 10.3 ka, before ice retreat began in Jakobshavn Isfjord and Sikujuitsoq Fjord, the margin retreated across Disko Bugt primarily via calving at ~ 110 m yr⁻¹ (Long and Roberts, 2003; Long et al., 2006). In Jakobshavn Isfjord itself, ¹⁰Be ages indicate that Jakobshavn Isbræ retreated through the entire length of the fjord between ~ 8.0 and 7.5 ka, at a rate of ~ 100 m yr⁻¹ (Young et al., 2011).

Modern retreat rates (since the Little Ice Age) in Jakobshavn Isfjord have been more rapid and variable. Retreat rates of the floating tongue of Jakobshavn Isbræ were erratic over the past ~ 150 years, and were punctuated by several episodes of rapid ice loss (Csatho et al., 2008). Significant retreat (~ 20 – 25 km) occurred between 1850 and 1946 (Csatho et al., 2008), yielding integrated retreat rates of ~ 200 – 250 m yr⁻¹. After a period of stability between 1946 and 1998, the floating tongue retreated another ~ 20 km between 1999 and 2004 (Csatho et al., 2008), yielding retreat rates over an order of magnitude faster than between 1850 and 1946. However, comparison between geologic and modern rates can be misleading, as the duration of observation at least in part controls the inferred rate of retreat (Gardner et al., 1987). It is possible that, in the early Holocene, Sikujuitsoq Fjord behaved in a similar fashion to Jakobshavn Isfjord today, alternating between rapid and slow retreat, and yielding longer-term integrated rates of ~ 100 m yr⁻¹.

The retreat rate we calculate for the ice margin in Sikujuitsoq Fjord falls in the mid-range of ice margin retreat rates that have been documented for large, high-latitude bodies of ice both in Greenland and elsewhere (Fig. 9). In Sisimiut Fjord (central western Greenland; Fig. 1), retreat rates were ~ 48 m yr⁻¹ between 12.4 and 8.3 ka, and ~ 18 m yr⁻¹ between 8.3 and 4.5 ka (Rinterknecht et al., 2009). During the collapse of the Laurentide Ice Sheet between 12.0 and 7.0 ka, retreat rates calculated from reduction in ice sheet area are ~ 260 m yr⁻¹, although these rates range from 80 to 360 m yr⁻¹ (Andrews, 1973). While numerous explanations exist for rapid retreat of the Laurentide Ice Sheet margin, it is likely that mass loss through calving of a marine-based margin played an important role, since $\sim 56\%$ of the former ice-covered area had become proglacial lake or sea (Andrews, 1973). On Baffin Island, a marine-based ice margin retreated at a minimum rate of ~ 58 m yr⁻¹ through Sam Ford Fjord ~ 9.5 ka, and then slowed to ~ 5 m yr⁻¹ when it became grounded at head of the fjord (Briner et al., 2009). Large, calving-dominated outlet glaciers in Alaska have exhibited very rapid retreat rates over the past 100 years, including 350 m yr⁻¹ for the McCarthy Glacier (Wiles and Calkin, 1993) and 500 m yr⁻¹ for the Icy Bay glacier system (Porter, 1989). However, comparison with these modern-day Alaskan glaciers may suffer from the same duration of observation bias described above.

The variability in ice margin retreat rates discussed above cannot be attributed to a single factor. This variability may be caused by retreat style (e.g. surface ablation versus calving), fjord geometry, ice flow patterns (e.g. influence from nearby ice streams), external forcings (e.g. warm ocean currents), or the duration of observation. The large temporal gap in between the two populations of data (Fig. 9) is likely because global ice cover was not

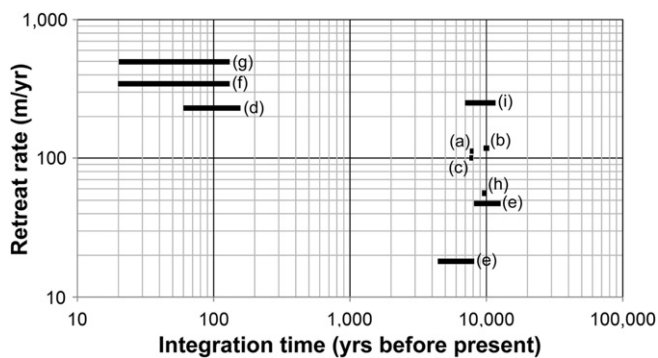


Fig. 9. Compilation of lateral ice margin retreat rates from studies that investigated large bodies of ice at high latitudes (see Section 5.6), including: (a) Sikujuitsoq Fjord, West Greenland (this study); (b) Disko Bugt, West Greenland (Long and Roberts, 2003); (c) Jakobshavn Isfjord, West Greenland (Young et al., 2011); (d) Jakobshavn Isfjord, West Greenland (Csatho et al., 2008); (e) Sisimiut Fjord, West Greenland (Rinterknecht et al., 2009); (f) McCarthy Glacier, Alaska, USA (Wiles and Calkin, 1993); (g) Icy Bay Glacier System, Alaska, USA (Porter, 1989); (h) Sam Ford Fjord, Baffin, Canada (Briner et al., 2009); and (i) Laurentide Ice Sheet, USA (Andrews, 1973).

rapidly declining in the middle and late Holocene, and ice margin retreat rates from this time period are underrepresented in the literature. Modern rates of ice margin retreat are appreciably higher than those in the early Holocene; however, it is not possible to determine whether this difference is due to the duration of observation bias or to real differences in climate forcings.

6. Conclusions

^{10}Be concentrations in bedrock and boulders near Sikujuitsoq Fjord reflect erosion efficiency over the last glaciation as well as the timing and process of deglaciation. Paired bedrock and boulder samples indicate that nuclides inherited from prior periods of cosmic-ray exposure are only present in bedrock exposed in the early Holocene and covered for too short a period later in the Holocene to erode the surface effectively. Otherwise, the large number of concordant bedrock and boulder ages indicate clearly that this area was subjected to subglacial erosion rates sufficiently high to remove at least several meters of rock between major interglaciations. Deglaciation in this region was punctuated by episodes of re-advance, resulting in a complex distribution of ^{10}Be concentrations; an initial episode of retreat exposed the outer land surface and some of the inner land surface $\sim 10.3 \pm 0.4$ ka ($n = 7$); a subsequent episode of retreat exposed the inner land surface $\sim 8.0 \pm 0.7$ ka ($n = 21$), after the deposition of the Fjord Stade moraine complex. The ice margin ultimately retreated behind the position of the historic moraine ~ 7.6 ka. Data from this study, as well as the spatial and altitudinal distribution of landscape features, suggest that ice surface lowering at each individual dipstick took place too rapidly to measure with ^{10}Be , likely within several hundred years. Lateral ice margin retreat was also rapid, at rates of ~ 100 m yr^{-1} . The data indicate that a rapid reorganization of the Jakobshavn Isbræ drainage took place during the early Holocene, following the abandonment of the Fjord Stade moraine complex. Comparison of data from Sikujuitsoq Fjord and Jakobshavn Isfjord suggests that retreat of Jakobshavn Isbræ set the timing and pace of deglaciation for the surrounding ice margin.

Acknowledgments

Support for this research was provided by National Science Foundation award number ARC-0713956 to Bierman and Neumann, NSF-0752848 to Briner, a National Science Foundation

Graduate Research Fellowship to Corbett, and the University of Vermont. Field support was provided by CH2MHILL. This work performed in part under the auspices of the US Department of Energy by Lawrence Livermore National Laboratory under contract DE-AC52-07NA27344. Thank you to R. Braucher and one anonymous reviewer for constructive comments.

References

- Alley, R., Anandakrishnan, S., Dupont, T., Parizek, B., Pollard, D., 2007. Effect of sedimentation on ice-sheet grounding-line stability. *Science* 315, 1838–1841.
- Alley, R., Andrews, J., Brigham-Grette, J., Clarke, G., Cuffey, K., Fitzpatrick, J., Funder, S., Marshall, S., Miller, G., Mitrovica, J., 2010. History of the Greenland ice sheet: paleoclimatic insights. *Quaternary Science Reviews* 29, 1728–1756.
- Alley, R., Mayewski, P., Sowers, T., Stuiver, M., Taylor, K., Clark, P., 1997. Holocene climatic instability: a prominent, widespread event 8200 yr ago. *Geology* 25, 483–486.
- Andrews, J., 1973. The Wisconsin Laurentide ice sheet: dispersal centers, problems of rates of retreat, and climatic implications. *Arctic and Alpine Research* 5, 185–199.
- Axford, Y., Briner, J., Miller, G., Francis, D., 2009. Paleocological evidence for abrupt cold reversals during peak Holocene warmth on Baffin Island, Arctic Canada. *Quaternary Research* 71, 142–149.
- Balco, G., 2011. Contributions and unrealized potential contributions of cosmogenic-nuclide exposure dating to glacier chronology, 1990–2010. *Quaternary Science Reviews* 30, 3–27.
- Balco, G., Briner, J., Finkel, R., Rayburn, J., Ridge, J., Schaefer, J., 2009. Regional beryllium-10 production rate calibration for late-glacial northeastern North America. *Quaternary Geochronology* 4, 93–107.
- Balco, G., Stone, J., Lifton, N., Dunai, T., 2008. A complete and easily accessible means of calculating surface exposure ages or erosion rates from ^{10}Be and ^{26}Al measurements. *Quaternary Geochronology* 3, 174–195.
- Bentley, C., 1987. Antarctic ice streams: a review. *Journal of Geophysical Research* 92, 8843–8858.
- Bierman, P., 1994. Using in situ produced cosmogenic isotopes to estimate rates of landscape evolution: a review from the geomorphic perspective. *Journal of Geophysical Research* 99, 13885–13896.
- Bierman, P., Marsella, K., Patterson, C., Davis, P., Caffee, M., 1999. Mid-pleistocene cosmogenic minimum-age limits for pre-Wisconsinan glacial surfaces in southwestern Minnesota and southern Baffin Island: a multiple nuclide approach. *Geomorphology* 27, 25–39.
- Bougamont, M., Tulaczyk, S., 2003. Glacial erosion beneath ice streams and ice stream tributaries: constraints on temporal and spatial distribution of erosion from numerical simulations of a West Antarctic ice stream. *Boreas* 32, 178–190.
- Briner, J., Bini, A., Anderson, R., 2009. Rapid early Holocene retreat of a Laurentide outlet glacier through an Arctic fjord. *Nature Geoscience* 2, 496–499.
- Briner, J., Miller, G., Davis, P., Bierman, P., Caffee, M., 2003. Last Glacial Maximum ice sheet dynamics in Arctic Canada inferred from young erratics perched on ancient tors. *Quaternary Science Reviews* 22, 437–444.
- Briner, J., Stewart, H., Young, N., Phillips, W., Losee, S., 2010. Using proglacial-threshold lakes to constrain fluctuations of the Jakobshavn Isbræ ice margin, western Greenland, during the Holocene. *Quaternary Science Reviews* 29, 3861–3874.
- Briner, J., Swanson, T., 1998. Using inherited cosmogenic ^{36}Cl to constrain glacial erosion rates of the Cordilleran ice sheet. *Geology* 26, 3–6.
- Corbett, L., Bierman, P., Graly, J., Neumann, T., Rood, D., Finkel, R., 2009. In situ cosmogenic ^{10}Be estimates of deglaciation timing and glacial erosion efficiency, western Greenland. *Geological Society of America Abstracts with Programs* 41, 621.
- Csatho, B., Schenk, T., Van der Veen, C., Krabill, W., 2008. Intermittent thinning of Jakobshavn Isbræ, west Greenland, since the little ice age. *Journal of Glaciology* 54, 131–144.
- Cuffey, K., Marshall, S., 2000. Substantial contribution to sea-level rise during the last interglacial from the Greenland ice sheet. *Nature* 404, 591–594.
- Dahl-Jensen, D., Mosegaard, K., Gundestrup, N., Clow, G., Johnsen, S., Hansen, A., Balling, N., 1998. Past temperatures directly from the Greenland ice sheet. *Science* 282, 268–271.
- Delmas, M., Gunnell, Y., Braucher, R., Calvet, M., Bourles, D., 2008. Exposure age chronology of the last glaciation in the eastern Pyrenees. *Quaternary Research* 69, 231–241.
- Fabel, D., Harbor, J., 1999. The use of in-situ produced cosmogenic radionuclides in glaciology and glacial geomorphology. *Annals of Glaciology* 28, 103–110.
- Gardner, T., Jorgensen, D., Shuman, C., Lemieux, C., 1987. Geomorphic and tectonic process rates: effects of measured time interval. *Geology* 15, 259–261.
- Gosse, J., Phillips, F., 2001. Terrestrial in situ cosmogenic nuclides: theory and application. *Quaternary Science Reviews* 20, 1475–1560.
- Häkansson, L., Alexanderson, H., Hjort, C., Moller, P., Briner, J., Aldahan, A., Possnert, G., 2008. Late Pleistocene glacial history of Jameson Land, central East Greenland, derived from cosmogenic ^{10}Be and ^{26}Al exposure dating. *Boreas* 38, 244–260.
- Harbor, J., Stroeven, A., Fabel, D., Clarhäll, A., Kleman, J., Li, Y., Elmore, D., Fink, D., 2006. Cosmogenic nuclide evidence for minimal erosion across two subglacial

- sliding boundaries of the late glacial Fennoscandian ice sheet. *Geomorphology* 75, 90–99.
- Heyman, J., Stroeven, A., Harbor, J., Caffee, M., 2010. Too young or too old: evaluating cosmogenic exposure dating based on an analysis of compiled boulder exposure ages. *Earth and Planetary Science Letters* 302, 71–80.
- Holland, D., Thomas, R., De Young, B., Ribergaard, M., Lyberth, B., 2008. Acceleration of Jakobshavn Isbræ triggered by warm subsurface ocean waters. *Nature Geoscience* 1, 659–664.
- Hunt, A., Larsen, J., Bierman, P., Petrucci, G., 2008. Investigation of factors that affect the sensitivity of accelerator mass spectrometry for cosmogenic ^{10}Be and ^{26}Al isotope analysis. *Analytical Chemistry* 80, 1656–1663.
- IPCC, 2007. *Climate Change 2007: The Physical Science Basis. Contribution of Working Group I to the Fourth Assessment Report of the Intergovernmental Panel on Climate Change*. Cambridge University Press.
- Kelly, M., Lowell, T., Hall, B., Schaefer, J., Finkel, R., Goehring, B., Alley, R., Denton, G., 2008. A ^{10}Be chronology of lateglacial and Holocene mountain glaciation in the Scoresby Sund region, east Greenland: implications for seasonality during lateglacial time. *Quaternary Science Reviews* 27, 2273–2282.
- Kohl, C., Nishiizumi, K., 1992. Chemical isolation of quartz for measurement of in-situ-produced cosmogenic nuclides. *Geochimica et Cosmochimica Acta* 56, 3583–3587.
- Lal, D., 1991. Cosmic ray labeling of erosion surfaces: in situ nuclide production rates and erosion models. *Earth and Planetary Science Letters* 104, 424–439.
- Letréguilly, A., Reeh, N., Huybrechts, P., 1991. The Greenland ice sheet through the last glacial-interglacial cycle. *Global and Planetary Change* 4, 385–394.
- Lilly, K., Fink, D., Fabel, D., Lambeck, K., 2010. Pleistocene dynamics of the interior of the East Antarctic ice sheet. *Geology* 38, 703–706.
- Lisiecki, L., Raymo, M., 2005. A Plio-Pleistocene stack of 57 globally distributed benthic ^{18}O records. *Paleoceanography* 20, 522–533.
- Lloyd, J., Park, L., Kuijpers, A., Moros, M., 2005. Early Holocene palaeoceanography and deglacial chronology of Disko Bugt, west Greenland. *Quaternary Science Reviews* 24, 1741–1755.
- Long, A., 2009. Back to the future: Greenland's contribution to sea-level change. *GSA Today* 19, 4–10.
- Long, A., Roberts, D., 2002. A revised chronology for the 'Fjord Stade' moraine in Disko Bugt, west Greenland. *Journal of Quaternary Science* 17, 561–579.
- Long, A., Roberts, D., 2003. Late Weichselian deglacial history of Disko Bugt, west Greenland, and the dynamics of the Jakobshavn Isbræ ice stream. *Boreas* 32, 208–226.
- Long, A., Roberts, D., Dawson, S., 2006. Early Holocene history of the west Greenland ice sheet and the GH-8.2 event. *Quaternary Science Reviews* 25, 904–922.
- Marquette, G., Gray, J., Gosse, J., Courchesne, F., Stockli, L., Macpherson, G., Finkel, R., 2004. Felsenmeer persistence under non-erosive ice in the Tornat and Kaumajet mountains, Quebec and Labrador, as determined by soil weathering and cosmogenic nuclide exposure dating. *Canadian Journal of Earth Sciences* 41, 19–38.
- Marsella, K., Bierman, P., Davis, P., Caffee, M., 2000. Cosmogenic ^{10}Be and ^{26}Al ages for the last glacial maximum, eastern Baffin Island, Arctic Canada. *Geological Society of America Bulletin* 112, 1296–1312.
- NASA Landsat Program, 2001. Landsat ETM+ scene p009r011_7dk20010707.742, SLC-On, USGS, Sioux Falls, 7/7/2001.
- Nishiizumi, K., Imamura, M., Caffee, M., Southon, J., Finkel, R., McAninch, J., 2007. Absolute calibration of ^{10}Be AMS standards. *Nuclear Instruments and Methods in Physics Research Section B: Beam Interactions with Materials and Atoms* 258, 403–413.
- Otto-Bliesner, B., Marshall, S., Overpeck, J., Miller, G., Hu, A., 2006. Simulating Arctic climate warmth and icefield retreat in the last interglaciation. *Science* 311, 1751–1753.
- Pallas, R., Rodes, A., Braucher, R., Carcaillet, J., Ortuno, M., Bordonau, J., Bourles, D., Vilaplana, J., Masana, E., Santanach, P., 2006. Late Pleistocene and Holocene glaciation in the Pyrenees: a critical review and new evidence from ^{10}Be exposure ages, south-central Pyrenees. *Quaternary Science Reviews* 25, 2937–2963.
- Phillips, F., Zreda, M., Smith, S., Elmore, D., Kubik, P., Sharma, P., 1990. Cosmogenic chlorine-36 chronology for glacial deposits at Bloody Canyon, eastern Sierra Nevada. *Science* 248, 1529–1532.
- Porter, S., 1989. Late Holocene fluctuations of the fiord glacier system in Icy Bay, Alaska, USA. *Arctic and Alpine Research* 21, 364–379.
- Rinterknecht, V., Gorokhovitch, Y., Schaefer, J., Caffee, M., 2009. Preliminary ^{10}Be chronology for the last deglaciation of the western margin of the Greenland Ice Sheet. *Journal of Quaternary Science* 24, 270–278.
- Roberts, D., Long, A., 2005. Streamlined bedrock terrain and fast ice flow, Jakobshavn Isbræ, West Greenland: implications for ice stream and ice sheet dynamics. *Boreas* 34, 25–42.
- Rood, D., Hall, S., Guilderson, T., Finkel, R., Brown, T., 2010. Challenges and opportunities in high-precision Be-10 measurements at CAMS. *Nuclear Instruments and Methods in Physics Research Section B: Beam Interactions with Materials and Atoms* 268, 730–732.
- Schildgen, T., Phillips, W., Purves, R., 2005. Simulation of snow shielding corrections for cosmogenic nuclide surface exposure studies. *Geomorphology* 64, 67–85.
- Smith, A., Murray, T., Nicholls, K., Makinson, K., Adalgeirsdottir, G., Behar, A., Vaughan, D., 2007. Rapid erosion, drumlin formation, and changing hydrology beneath an Antarctic ice stream. *Geology* 35, 127–130.
- Smith, J., Finkel, R., Farber, D., Rodbell, D., Seltzer, G., 2005. Moraine preservation and boulder erosion in the tropical Andes: interpreting old surface exposure ages in glaciated valleys. *Journal of Quaternary Science* 20, 735–758.
- Stone, J., 2000. Air pressure and cosmogenic isotope production. *Journal of Geophysical Research* 105, 23753–23759.
- Stone, J., Balco, G., Sugden, D., Caffee, M., Sass III, L., Cowdery, S., Siddoway, C., 2003. Holocene deglaciation of Marie Byrd land, west Antarctica. *Science* 299, 99–102.
- Stroeven, A., Fabel, D., Hättestrand, C., Harbor, J., 2002. A relict landscape in the centre of Fennoscandian glaciation: cosmogenic radionuclide evidence of tors preserved through multiple glacial cycles. *Geomorphology* 44, 145–154.
- Sugden, D., Balco, G., Cowdery, S., Stone, J., Sass III, L., 2005. Selective glacial erosion and weathering zones in the coastal mountains of Marie Byrd Land, Antarctica. *Geomorphology* 67, 317–334.
- Vinther, B., Buchardt, S., Clausen, H., Dahl-Jensen, D., Johnsen, S., Fisher, D., Koerner, R., Raynaud, D., Lipenkov, V., Andersen, K., 2009. Holocene thinning of the Greenland ice sheet. *Nature* 461, 385–388.
- Weidick, A., 1968. Observations on some Holocene glacier fluctuations in West Greenland. *Meddelelser Om Gronland* 165 (6), 194.
- Weidick, A., Bennike, O., 2007. Quaternary glaciation history and glaciology of Jakobshavn Isbræ and the Disko Bugt region, west Greenland: a review. *Geologic Survey of Denmark and Greenland Bulletin* 14, 1–13.
- Weidick, A., Oerter, H., Reeh, N., Thomsen, H., Thorning, L., 1990. The recession of the Inland ice margin during the Holocene climatic optimum in the Jakobshavn Isfjord area of west Greenland. *Global and Planetary Change* 2, 389–399.
- Wiles, G., Calkin, P., 1993. Neoglacial fluctuations and sedimentation of an iceberglaciating glacier resolved with tree rings (Kenai Fjords National Park, Alaska). *Quaternary International* 18, 35–42.
- Young, N., Briner, J., Stewart, H., Axford, Y., Csatho, B., Rood, D., Finkel, R., 2011. Response of Jakobshavn Isbræ, Greenland, to Holocene climate change. *Geology* 39, 131–134.